

# Semi-annihilating $Z_3$ Dark Matter for XENON1T Excess

P. Ko<sup>(a)</sup> and Yong Tang<sup>(b,c,d,e)</sup>

<sup>a</sup>*Korea Institute for Advanced Study, Seoul 02445, South Korea*

<sup>b</sup>*School of Astronomy and Space Sciences,*

*University of Chinese Academy of Sciences (UCAS), Beijing 100049, China*

<sup>c</sup>*National Astronomical Observatories, Chinese Academy of Sciences, Beijing 100101, China*

<sup>d</sup>*School of Fundamental Physics and Mathematical Sciences,*

*Hangzhou Institute for Advanced Study, UCAS, Hangzhou 310024, China*

<sup>e</sup>*International Centre for Theoretical Physics Asia-Pacific, Beijing/Hangzhou, China*

## Abstract

The recently reported result from XENON1T experiment indicates that there is an excess with  $3.5\sigma$  significance in the electronic recoil events. Interpreted as new physics, new sources are needed to account for the electronic scattering. Here, we show that a dark fermion  $\psi$  from semi-annihilation of  $Z_3$  dark matter  $X$  and subsequent decay may be responsible for the excess. The relevant semi-annihilation process is  $X + X \rightarrow \bar{X} + V_\mu (\rightarrow \psi + \bar{\psi})$ , in which the final  $\psi$  has a box-shape energy spectrum. The fast-moving  $\psi$  can scatter with electron through an additional gauge boson that mixes with photon kinetically. The shape of the signals in this model can be well consistent with the observed excess.

## I. INTRODUCTION

Recently, XENON1T collaboration has reported an excess with  $3.5\sigma$  significance in the electronic recoil events with an exposure of 0.65 tonne-year [1] data. The excess is observed around energy range  $2 - 3$  keV, which could be the relevant range for solar axion search <sup>1</sup>. However, the interpretation of vanilla solar axion is in strong conflict with other astrophysical bounds on stellar cooling [4–7]. Alternative explanations are then needed for such an excess.

Although the conservative scenario with tritium can not be excluded or confirmed at the moment, various relevant interpretations of new physics, constraints and connections have been explored timely in [8–43]. For instance, the excess could be connected to the absorption of bosonic dark matter [8–11] (axion-like particle and dark photon), boosted dark matter [12–15], inelastic scattering [16–18, 42, 43].

In this study, we present an explanation of the excess in the framework of semi-annihilating dark matter with  $Z_3$  symmetry. The model was originally proposed and investigated in different contexts [44, 45] by the present authors. Here, we show that in different parameter space, the semi-annihilation of dark matter can provide an unstable gauge boson that decays into a pair of dark fermion. The resulting boosted dark fermions can then interact with the electrons through dark photon with kinetic mixing and induce the electronic recoil signals. The event spectrum can be well consistent with the XENON1T observation. We also put an upper bound on the semi-annihilation cross section of dark matter and lower bound on the the electron-scattering cross section.

This paper is organized as follows. In Sec. II we present the model setup by introducing the particle contents and Lagrangian. Then in Sec. III we discuss the detailed kinematics that would be relevant for later investigations. Later, we give both analytic estimation and numerical illustration how the signal in this model can fit the XENON1T excess in Sec. IV and present constraints on the relevant cross sections in Sec V. Finally, we summarize our paper.

---

<sup>1</sup> This search also has some implications for neutrino magnetic moment, see Refs. [1–3].

TABLE I.  $U(1)_D \times U(1)'_D$  charge assignments of the fields

Fields	$X$	$\Phi$	$\psi$
$U(1)_D$ charges	3	1	$Q_\psi$
$U(1)'_D$ charges	0	0	1

## II. THE MODEL

The Lagrangian we are considering is the following one with 2 complex scalars  $X$  and  $\Phi$ , a fermion  $\psi$ , and two dark  $U(1)_D \times U(1)'_D$  gauge groups with two dark gauge bosons,  $V_\mu$  for  $U(1)_D$  and  $A'_\mu$  for  $U(1)'_D$ :

$$\begin{aligned} \mathcal{L} \supset & (D_\mu X)^\dagger D^\mu X + (D_\mu \Phi)^\dagger D^\mu \Phi - \lambda_X (\Phi^\dagger X^3 + \Phi X^{\dagger 3}) - \bar{\psi} (i\gamma^\mu D_\mu - m_\psi) \psi \\ & - \frac{1}{4} V_{\mu\nu} V^{\mu\nu} - \frac{1}{4} F'_{\mu\nu} F'^{\mu\nu} - \frac{1}{2} m_{A'}^2 A'_\mu A'^\mu - \frac{\epsilon}{2} F'_{\mu\nu} F^{\mu\nu} - V(X, \Phi, H), \end{aligned} \quad (1)$$

The charges assignments of these fields are listed in TABLE I. Here the covariant derivatives are defined as

$$D_\mu X = (\partial_\mu - igV_\mu)X, \quad D_\mu \Phi = (\partial_\mu - i3gV_\mu)\Phi, \quad D_\mu \psi = (\partial_\mu - igQ_\psi V_\mu - ifA'_\mu)\psi,$$

with  $g$  and  $f$  are the gauge couplings for  $U(1)_D$  and  $U(1)'_D$ , respectively. Here we have assigned the  $U(1)_D$  charges of  $X$  and  $\Phi$  to be 1 and 3, respectively. They are neutral under  $U(1)'_D$  however. The fermion  $\psi$  may have a different  $U(1)_D$  charge  $Q_\psi$ , but should also be charged under  $U(1)'_D$ . The  $U(1)'_D$  gauge field  $A'_\mu$  has the kinetic mixing with ordinary photon  $A_\mu$ , and will induce  $\psi$ -electron scattering for XENON1T excess. The mass of  $A'$  can originate the usual Higgs mechanism or Stückelberg trick, which does not affect our discussions in this paper.  $A'$  may be connected to other hidden sector, which would relax its experimental constraints. Different implementations of  $Z_3$  symmetry in other contexts have been investigated in [46–57].

After the spontaneous symmetry breaking of  $U(1)_D$ , the scalar  $\Phi$  has a non-zero vacuum expectation value  $v_\phi$ ,  $\Phi \rightarrow (v_\phi + \phi)/\sqrt{2}$ , and the gauge field  $V_\mu$  gets its mass. In the scalar potential we also have the cubic term  $(X^3 + X^{\dagger 3})$  that preserves the discrete  $Z_3$  symmetry,  $X \rightarrow \exp(i2n\pi/3)X$ , which makes  $X$  a stable dark matter candidate but have the semi-annihilating process with emission of  $V_\mu$  or (dark) Higgs (see Refs. [44, 45] for more detail).

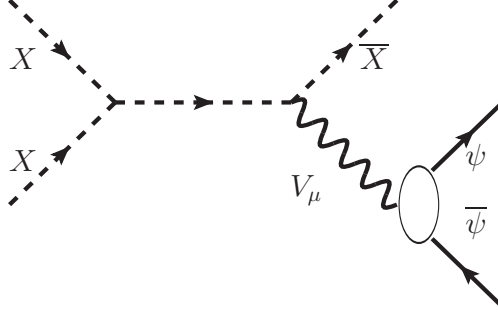


FIG. 1. The typical Feynman diagram of semi-annihilation process,  $X + X \rightarrow \bar{X} + V_\mu$ , with subsequent on-shell decay  $V_\mu \rightarrow \psi + \bar{\psi}$ .

The masses and interaction terms of scalar fields are included collectively in the potential  $V(X, \Phi, H)$ , where  $H$  is the Higgs doublet in standard model. Interaction with  $H$  can make the dark sector in contact with thermal bath, which would be needed for thermal production of  $X$ . For non-thermal production, we do not have to specify the form and strength in  $V(X, \Phi, H)$ .

### III. KINEMATICS

The relevant semi-annihilation process is shown in Fig. 1,

$$X + X \rightarrow \bar{X} + V_\mu (\rightarrow \psi \bar{\psi}), \quad (2)$$

where the dark matter  $X$  with  $Z_3$  symmetry semi-annihilates into its antiparticle and a dark photon  $V_\mu$  which decays into dark  $\psi$  pair subsequently. Choosing the mass differences properly, the resulting  $\psi$  with velocity  $v_\psi \sim 0.1c$  is the boosted dark fermion that interacts with electron by an additional gauge interaction  $A'_\mu$  that mixes photon through kinetic term. Here, we focus on the phenomenology in XENON1T. General discussions about boosted dark matter in other context can be found in [58–63].

In principle, there is another annihilation process  $X + \bar{X} \rightarrow V_\mu^* \rightarrow \psi + \bar{\psi}$  where we have the corresponding energy and velocity,

$$E_\psi \simeq m_X, \text{ and } v_\psi = \sqrt{1 - \frac{m_\psi^2}{m_X^2}}. \quad (3)$$

Here and after,  $m_i, i = X, V, \psi$  are the masses for particles,  $X, V_\mu, \psi$ , respectively. Simple estimation implies that we have  $v_\psi \sim 0.1c$  for  $m_\psi \simeq 0.995m_X$ , and  $v_\psi \sim 0.87c$  for  $m_\psi \simeq$

$0.5m_X$ . However, this process is velocity suppressed at the present time when dark matter in the Milky way is moving with velocity  $v \sim 10^{-3}c$ , and the cross section would be  $\sim 10^{-6}$  smaller than that in semi-annihilation. Therefore, we shall not consider this channel in our later discussions.

There are also contributions from annihilation  $X + \bar{X} \rightarrow V_\mu + V_\mu$ , whose cross section depends on the gauge coupling  $\sim g^4$ , in comparison with that for the semi-annihilation  $\sim g^2\lambda_X^2$ . For simplicity, we shall focus on the parameter region  $\lambda_X \gg g$  such that the semi-annihilation always dominates in our later discussions. Note that the opposite limit  $\lambda_X \ll g$  would make  $X + \bar{X} \rightarrow V_\mu + V_\mu$  dominant, which also works with the boosted  $V_\mu$  that decays, although with a different kinematics <sup>2</sup>.

In the semi-annihilation we have the relations for the energies of final states,

$$E_V = \frac{3m_X^2 + m_V^2}{4m_X}, E_X = \frac{5m_X^2 - m_V^2}{4m_X}. \quad (4)$$

The velocity of  $V_\mu$  is

$$v_V = \frac{1}{4m_V m_X} \sqrt{[4m_X^2 - (m_X + m_V)^2] [4m_X^2 - (m_X - m_V)^2]}. \quad (5)$$

The final  $\psi$  particles have an energy distribution with box shape,

$$2 = \int_{E_-}^{E_+} dE \frac{dN}{dE}, \quad \frac{dN}{dE} = \frac{2}{E_+ - E_-} \theta(E_-, E_+), \quad (6)$$

where  $\theta(E_-, E_+) = 1$  for  $E_- < E < E_+$  and zero otherwise,  $E_\pm = E_V (1 \pm \beta_V \beta_\psi^*) / 2$ ,  $\beta_V = \sqrt{1 - m_V^2/m_X^2}$  and  $\beta_\psi^* = \sqrt{1 - 4m_\psi^2/m_V^2}$ . It can be also translated into velocity distribution  $f_\psi$ ,

$$2 = \int_{v_-}^{v_+} dv_\psi f_\psi, \quad f_\psi = \frac{2m_\psi v_\psi}{(E_+ - E_-) (1 - v_\psi^2)^{3/2}}, \quad (7)$$

where  $v_\psi = \sqrt{1 - m_\psi^2/E_\psi^2}$ . The energy interval of the distribution is  $E_V \beta_V \beta_\psi^*$ , which depends on the three masses, and the relative half-width is  $\delta = \beta_V \beta_\psi^*$ . For small mass differences,  $m_X - m_V \ll m_V$  and/or  $m_V/2 - m_\psi \ll m_\psi$ , the spectrum will be very narrow around  $E_V/2$ .

#### IV. EVENT RATE

The fast-moving  $\psi$  can scatter with electron through  $A'_\mu$  interaction and induce prompt scintillation events (S1) at XENON1T experiment. The recoil energy of electron is  $E_R \simeq$

<sup>2</sup> In Ref. [45], this channel was exploited to explain galactic center  $\gamma$ -ray excess assuming  $m_V \lesssim m_X$ .

$2m_e v_\psi^2$  for  $m_\psi \gg m_e$ . Since the events of excess are centered around  $E_R \sim 2.5\text{keV}$ , we would need  $v_\psi \simeq 0.05c$ . The differential rate of such events can be estimated as

$$\frac{dR}{dE} = n_T \langle \Phi_\psi \sigma_e(E) \rangle, \quad (8)$$

where  $n_T \sim 4.6 \times 10^{27}/\text{ton}$ ,  $\Phi_\psi$  is the flux of  $\psi$  and  $\sigma_e$  is the scattering cross section between  $\psi$  and electron. To explain the excess, we would need  $dR/dE \sim 30/(\text{ton yr keV})$ , which gives

$$\langle \Phi_\psi \sigma_e \rangle \simeq 2.4 \times 10^{-35}/(\text{s keV}). \quad (9)$$

The  $\langle \cdot \rangle$  denotes that we shall take into account the smearing effect due to energy resolution and efficiency of the experiments [1]. The energy resolution [64] is parametrized by Gaussian distribution with uncertainty  $\sigma$ ,

$$\frac{\sigma}{E} = \left( \frac{31.71}{\sqrt{E}} + 0.15 \right) \%. \quad (10)$$

For the reconstructed energy at  $E \simeq 2.7\text{keV}$ , the relative resolution is about 19.45%. All of these effects are included in our later numerical illustrations.

The flux  $\Phi_\psi$  from annihilation of dark matter of our galaxy is given by

$$\begin{aligned} \Phi_\psi &= \frac{v_\psi}{4\pi} \frac{dN}{dE} \frac{\langle \sigma_{\text{ann}} v \rangle}{4} \int d\Omega \int ds \frac{\rho_X^2}{m_X^2} \\ &\simeq 10^{-5} \text{cm}^{-2} \text{s}^{-1} \times \left( \frac{\text{GeV}}{m_X} \right)^2 \left( \frac{\langle \sigma_{\text{ann}} v \rangle}{3 \times 10^{-26} \text{cm}^3/\text{s}} \right) \left( \frac{v_\psi}{0.05c} \right) \frac{dN}{dE}, \end{aligned} \quad (11)$$

where the  $\rho_X$  is the energy density of  $X$  with an NFW profile,  $dN/dE$  is the number distribution of  $\psi$  at production and the integration is performed over the light-of-sight  $s$  and all-sky solid angle  $\Omega$ .

The above analytic estimation shows that the  $\psi$ - $e$  scattering cross section should be around  $\sigma_e \sim 10^{-30} \text{cm}^2$  for GeV-scale dark matter with canonically thermal annihilation cross section. Increasing the mass of dark matter would decrease the flux of  $\psi$  and correspondingly requires larger scattering cross section  $\sigma_e$  for compensation of the flux loss.

In Fig. (2) we illustrate with a box-shape energy spectrum having relative half-width,  $\delta = 0.1\%$ . The central value of recoil energy is chosen at  $E_R \simeq 2.7\text{keV}$ . The black dots with error bars and the gray background curve are extracted from XENON1T result [1]. The dotted curve describes the signal shapes with  $\delta = 0.1\%$  and the dashed curve is the sum of background and signal. Apparently, the signal can give a consistent fit to the reported

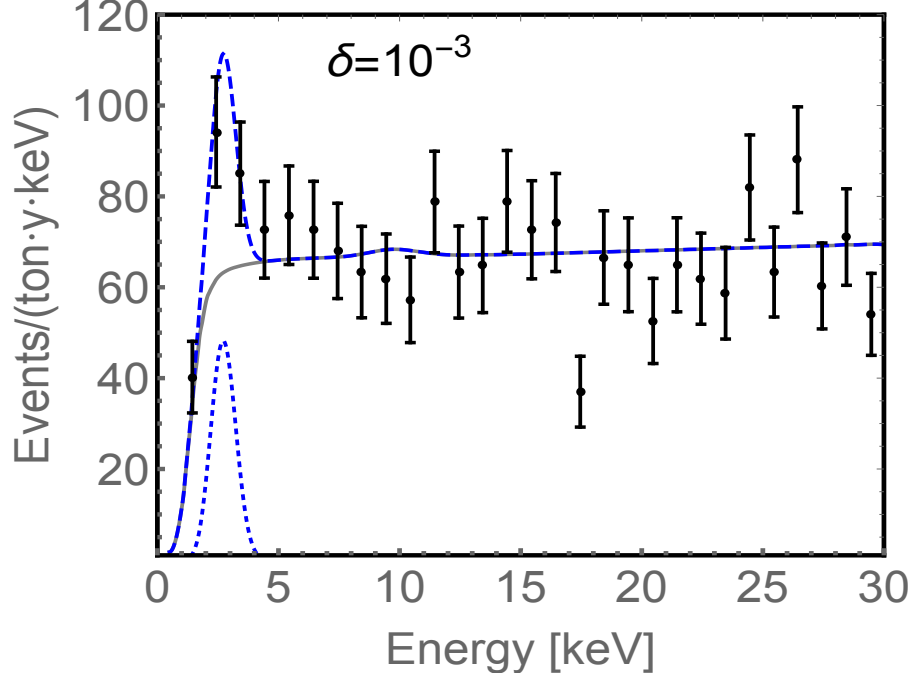


FIG. 2. The illustration of signal shapes with box-shape spectra for boosted  $\psi$  from  $V_\mu$ 's decay. The relative half-width is taken as  $\delta = 0.1\%$ , shown as the dotted curves. The black dots with error bars and the gray background curved are extracted from XENON1T results. The central value of the recoil energy is chosen at  $E_R \simeq 2.7$  keV.

excess. The value of  $\delta$  then can be directly translated into the requirements on the mass differences through the relation  $\delta = \beta_V \beta_\psi^*$ . Together with  $v_\psi \simeq 0.05c$ , we can determine the two mass ratios of  $m_V/m_X$  and  $m_\psi/m_V$ .

To precisely determine the favored parameter region, dedicated statistical analysis would be needed and is beyond the scope of this paper. Instead, we only show several contours for the relative ratios of  $m_V/m_X$  and  $m_\psi/m_V$  in Fig. 3 to provide the proof of concept. The three straight lines in the figure correspond to the different velocities of  $v_\psi = 0.01, 0.05, 0.1c$  (from top to down) and the numbers near the three blue curves indicates the relative half-width  $\delta = 0.1\%, 0.5\%, 1\%$  (from top to down), respectively. The choice of  $v_\psi \simeq 0.05c$  would suggest  $\delta \simeq 0.1\%$ ,  $m_V/m_X \simeq 0.998$  and  $m_\psi/m_V \simeq 0.499$ . And more conservative values of  $v_\psi \simeq 0.1c$  can enlarge the available parameter space significantly and make  $\delta \sim 0.5\%$  viable.

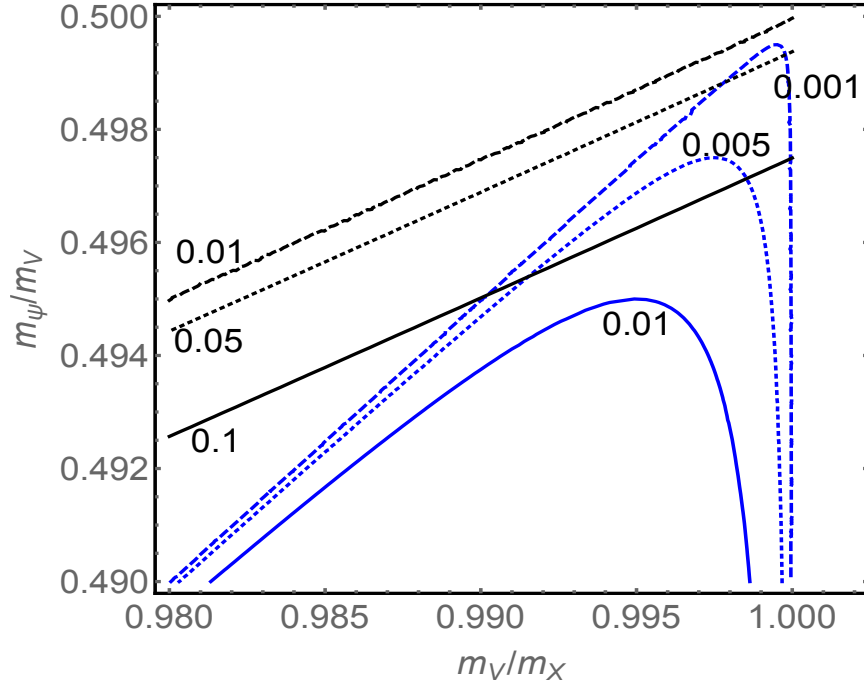


FIG. 3. The three straight lines correspond to the velocity of  $\psi$ ,  $v_\psi = 0.01c$  (dash),  $0.05c$  (dot),  $0.1c$  (solid). The three blue curves are the contours for relative half-width  $\delta = 0.001$  (dash),  $0.005$  (dot),  $0.01$  (solid).

## V. CONSTRAINTS

As we have demonstrated in previous sections, the event rate depends on the product of the dark matter semi-annihilation cross section and  $\psi$ - $e$  scattering cross section,  $\langle\sigma_{\text{ann}}v\rangle\sigma_e$ . Larger  $\langle\sigma_{\text{ann}}v\rangle$  implies smaller  $\sigma_e$ . There would be some degeneracy in these two values.

However, there is an upper bound on  $\langle\sigma_{\text{ann}}v\rangle$  from astrophysics even if all the final annihilation products are in dark sector. Because the resulting  $X$  from semi-annihilation is also fast moving and may escape from the dark halo in our galaxy, we should require the annihilation rate is smaller than 1 per Hubble time, then we obtain the upper bound,

$$\frac{\langle\sigma_{\text{ann}}v\rangle}{m_X} \lesssim 3 \times 10^{-18} \frac{\text{cm}^3/\text{s}}{\text{GeV}}. \quad (12)$$

We should note that if  $\langle\sigma_{\text{ann}}v\rangle \gg 3 \times 10^{-26} \text{cm}^3/\text{s}$ ,  $X$  can not be produced thermally in the early universe since its relic density would be too small. In such a case, other production mechanism would be needed. For instance,  $X$  could be produced from other heavy particles's decay, or was never in thermal equilibrium due to low reheating temperature after inflation.

In order to explain the XENON1T excess, the above upper bound correspondingly gives a lower bound on  $\sigma_e$ ,

$$\sigma_e \gtrsim 10^{-38} \text{cm}^2 \times \frac{m_X}{\text{GeV}}. \quad (13)$$

This limit can be easily satisfied for GeV-scale dark matter as we shall show below. Note that the constraints from cosmic-ray scattering with dark matter [65, 66] do not apply here because the density of  $\psi$  particles in the galactic background is much lower than dark matter  $X$ . If the Higgs-portal and  $V_\mu$  kinetic portal couplings are small, then the interaction between  $X$  and standard model particles would also be suppressed, therefore the scattering between  $X$  and cosmic rays is rare and the constraints can be relaxed, but potentially detectable in future.

The above requirement of  $\sigma_e$  can be satisfied with a viable kinetic mixing parameter  $\epsilon$  for  $\gamma - A'$  and dark photon mass  $m_{A'}$ ,

$$\sigma_e \simeq 4\pi\epsilon^2 \frac{\alpha\alpha' m_e^2}{m_{A'}^4} \simeq 1.0 \times 10^{-31} \text{cm}^2 \left( \frac{\epsilon^2}{10^{-8}} \right) \left( \frac{\alpha'}{10^{-2}} \right) \left( \frac{\text{MeV}}{m_{A'}} \right)^4. \quad (14)$$

Here  $\alpha$  is the fine-structure constant  $\alpha = 1/137$  and  $\alpha' = f^2/4\pi$  is the constant for  $A'$ . Such a light  $A'$  can be searched in various experiments. For the MeV-scale  $A'$  that mainly decays into invisible particles, the experimental constraints [67] allow  $\epsilon \lesssim 10^{-4}$ . The condition of Eq. (13) still holds even if we have  $\epsilon \sim 10^{-7}$ , a value well below the current limit.

## VI. SUMMARY

In this paper, we have presented an explanation of the recently observed excess in electronic recoil events at XENON1T experiment with a dark matter model with local  $Z_3$  discrete symmetry. The semi-annihilation of dark matter  $X$  can provide an unstable gauge boson  $V_\mu$  which subsequently decays into dark fermion pair  $\psi + \bar{\psi}$ . The energy spectrum of dark fermion has a box shape, with the width depending on the relative mass differences. Because of the semi-annihilation and decay,  $X + X \rightarrow \bar{X} + V_\mu (\rightarrow \psi + \bar{\psi})$ , the final dark fermion can be fast-moving with velocity around 0.05c. Then it scatters with an electron through the dark photon that has kinetic mixing with ordinary photon field. We have shown the resulting spectrum shape can be well consistent with the observed data by XENON1T with viable parameter values.

## Acknowledgments

The work of P.K. is supported in part by KIAS Individual Grant (Grant No. PG021403) at Korea Institute for Advanced Study and by National Research Foundation of Korea (NRF) Grant No. NRF-2019R1A2C3005009, funded by the Korea government (MSIT). YT is supported by National Natural Science Foundation of China (NSFC) under Grants No. 11851302.

- 
- [1] E. Aprile *et al.* (XENON), (2020), [arXiv:2006.09721 \[hep-ex\]](#).
  - [2] N. F. Bell, V. Cirigliano, M. J. Ramsey-Musolf, P. Vogel, and M. B. Wise, *Phys. Rev. Lett.* **95**, 151802 (2005), [arXiv:hep-ph/0504134](#).
  - [3] N. F. Bell, M. Gorchtein, M. J. Ramsey-Musolf, P. Vogel, and P. Wang, *Phys. Lett. B* **642**, 377 (2006), [arXiv:hep-ph/0606248](#).
  - [4] N. Viaux, M. Catelan, P. B. Stetson, G. Raffelt, J. Redondo, A. A. R. Valcarce, and A. Weiss, *Phys. Rev. Lett.* **111**, 231301 (2013), [arXiv:1311.1669 \[astro-ph.SR\]](#).
  - [5] A. Ayala, I. Domínguez, M. Giannotti, A. Mirizzi, and O. Straniero, *Phys. Rev. Lett.* **113**, 191302 (2014), [arXiv:1406.6053 \[astro-ph.SR\]](#).
  - [6] M. M. Miller Bertolami, B. E. Melendez, L. G. Althaus, and J. Isern, *JCAP* **10**, 069 (2014), [arXiv:1406.7712 \[hep-ph\]](#).
  - [7] M. Giannotti, I. G. Irastorza, J. Redondo, A. Ringwald, and K. Saikawa, *JCAP* **10**, 010 (2017), [arXiv:1708.02111 \[hep-ph\]](#).
  - [8] F. Takahashi, M. Yamada, and W. Yin, (2020), [arXiv:2006.10035 \[hep-ph\]](#).
  - [9] G. Alonso-Álvarez, F. Ertas, J. Jaeckel, F. Kahlhoefer, and L. Thormaehlen, (2020), [arXiv:2006.11243 \[hep-ph\]](#).
  - [10] K. Nakayama and Y. Tang, (2020), [arXiv:2006.13159 \[hep-ph\]](#).
  - [11] H. An, M. Pospelov, J. Pradler, and A. Ritz, (2020), [arXiv:2006.13929 \[hep-ph\]](#).
  - [12] K. Kannike, M. Raidal, H. Veermäe, A. Strumia, and D. Teresi, (2020), [arXiv:2006.10735 \[hep-ph\]](#).
  - [13] B. Fornal, P. Sandick, J. Shu, M. Su, and Y. Zhao, (2020), [arXiv:2006.11264 \[hep-ph\]](#).
  - [14] M. Du, J. Liang, Z. Liu, V. Q. Tran, and Y. Xue, (2020), [arXiv:2006.11949 \[hep-ph\]](#).

- [15] Y. Chen, J. Shu, X. Xue, G. Yuan, and Q. Yuan, (2020), [arXiv:2006.12447 \[hep-ph\]](#).
- [16] L. Su, W. Wang, L. Wu, J. M. Yang, and B. Zhu, (2020), [arXiv:2006.11837 \[hep-ph\]](#).
- [17] H. M. Lee, (2020), [arXiv:2006.13183 \[hep-ph\]](#).
- [18] Y. Jho, J.-C. Park, S. C. Park, and P.-Y. Tseng, (2020), [arXiv:2006.13910 \[hep-ph\]](#).
- [19] I. M. Bloch, A. Caputo, R. Essig, D. Redigolo, M. Sholapurkar, and T. Volansky, (2020), [arXiv:2006.14521 \[hep-ph\]](#).
- [20] R. Budnik, H. Kim, O. Matsedonskyi, G. Perez, and Y. Soreq, (2020), [arXiv:2006.14568 \[hep-ph\]](#).
- [21] K. Harigaya, Y. Nakai, and M. Suzuki, (2020), [arXiv:2006.11938 \[hep-ph\]](#).
- [22] A. Bally, S. Jana, and A. Trautner, (2020), [arXiv:2006.11919 \[hep-ph\]](#).
- [23] C. Boehm, D. G. Cerdeno, M. Fairbairn, P. A. Machado, and A. C. Vincent, (2020), [arXiv:2006.11250 \[hep-ph\]](#).
- [24] A. N. Khan, (2020), [arXiv:2006.12887 \[hep-ph\]](#).
- [25] R. Primulando, J. Julio, and P. Uttayarat, (2020), [arXiv:2006.13161 \[hep-ph\]](#).
- [26] Q.-H. Cao, R. Ding, and Q.-F. Xiang, (2020), [arXiv:2006.12767 \[hep-ph\]](#).
- [27] G. Paz, A. A. Petrov, M. Tammaro, and J. Zupan, (2020), [arXiv:2006.12462 \[hep-ph\]](#).
- [28] D. Aristizabal Sierra, V. De Romeri, L. Flores, and D. Papoulias, (2020), [arXiv:2006.12457 \[hep-ph\]](#).
- [29] J. Buch, M. A. Buen-Abad, J. Fan, and J. S. C. Leung, (2020), [arXiv:2006.12488 \[hep-ph\]](#).
- [30] M. Baryakhtar, A. Berlin, H. Liu, and N. Weiner, (2020), [arXiv:2006.13918 \[hep-ph\]](#).
- [31] J. Bramante and N. Song, (2020), [arXiv:2006.14089 \[hep-ph\]](#).
- [32] G. Choi, M. Suzuki, and T. T. Yanagida, (2020), [arXiv:2006.12348 \[hep-ph\]](#).
- [33] N. F. Bell, J. B. Dent, B. Dutta, S. Ghosh, J. Kumar, and J. L. Newstead, (2020), [arXiv:2006.12461 \[hep-ph\]](#).
- [34] U. K. Dey, T. N. Maity, and T. S. Ray, (2020), [arXiv:2006.12529 \[hep-ph\]](#).
- [35] L. Di Luzio, M. Fedele, M. Giannotti, F. Mescia, and E. Nardi, (2020), [arXiv:2006.12487 \[hep-ph\]](#).
- [36] M. Lindner, Y. Mambrini, T. B. de Melo, and F. S. Queiroz, (2020), [arXiv:2006.14590 \[hep-ph\]](#).
- [37] C. Gao, J. Liu, L.-T. Wang, X.-P. Wang, W. Xue, and Y.-M. Zhong, (2020), [arXiv:2006.14598 \[hep-ph\]](#).

- [38] L. Zu, G.-W. Yuan, L. Feng, and Y.-Z. Fan, (2020), [arXiv:2006.14577 \[hep-ph\]](#).
- [39] D. McKeen, M. Pospelov, and N. Raj, (2020), [arXiv:2006.15140 \[hep-ph\]](#).
- [40] J. Smirnov and J. F. Beacom, (2020), [arXiv:2002.04038 \[hep-ph\]](#).
- [41] M. Chala and A. Titov, (2020), [arXiv:2006.14596 \[hep-ph\]](#).
- [42] H. An and D. Yang, (2020), [arXiv:2006.15672 \[hep-ph\]](#).
- [43] S. Baek, J. Kim, and P. Ko, (2020), [arXiv:2006.16876 \[hep-ph\]](#).
- [44] P. Ko and Y. Tang, [JCAP \*\*1405\*\*, 047 \(2014\)](#), [arXiv:1402.6449 \[hep-ph\]](#).
- [45] P. Ko and Y. Tang, [JCAP \*\*1501\*\*, 023 \(2015\)](#), [arXiv:1407.5492 \[hep-ph\]](#).
- [46] G. Bélanger, K. Kannike, A. Pukhov, and M. Raidal, [JCAP \*\*1406\*\*, 021 \(2014\)](#), [arXiv:1403.4960 \[hep-ph\]](#).
- [47] M. Aoki and T. Toma, [JCAP \*\*1409\*\*, 016 \(2014\)](#), [arXiv:1405.5870 \[hep-ph\]](#).
- [48] N. Bernal, C. Garcia-Cely, and R. Rosenfeld, [JCAP \*\*1504\*\*, 012 \(2015\)](#), [arXiv:1501.01973 \[hep-ph\]](#).
- [49] S.-M. Choi and H. M. Lee, [JHEP \*\*09\*\*, 063 \(2015\)](#), [arXiv:1505.00960 \[hep-ph\]](#).
- [50] E. Ma, N. Pollard, R. Srivastava, and M. Zakeri, [Phys. Lett. \*\*B750\*\*, 135 \(2015\)](#), [arXiv:1507.03943 \[hep-ph\]](#).
- [51] Y. Cai and A. P. Spray, [JHEP \*\*06\*\*, 156 \(2016\)](#), [arXiv:1511.09247 \[hep-ph\]](#).
- [52] R. Ding, Z.-L. Han, Y. Liao, and W.-P. Xie, [JHEP \*\*05\*\*, 030 \(2016\)](#), [arXiv:1601.06355 \[hep-ph\]](#).
- [53] A. Hektor, A. Hryczuk, and K. Kannike, [JHEP \*\*03\*\*, 204 \(2019\)](#), [arXiv:1901.08074 \[hep-ph\]](#).
- [54] Z. Kang, P. Ko, and T. Matsui, [JHEP \*\*02\*\*, 115 \(2018\)](#), [arXiv:1706.09721 \[hep-ph\]](#).
- [55] P. Athron, J. M. Cornell, F. Kahlhoefer, J. McKay, P. Scott, and S. Wild, [Eur. Phys. J. \*\*C78\*\*, 830 \(2018\)](#), [arXiv:1806.11281 \[hep-ph\]](#).
- [56] K. Kannike, K. Loos, and M. Raidal, [Phys. Rev. \*\*D101\*\*, 035001 \(2020\)](#), [arXiv:1907.13136 \[hep-ph\]](#).
- [57] S.-M. Choi, J. Kim, H. M. Lee, and B. Zhu, [JHEP \*\*06\*\*, 135 \(2020\)](#), [arXiv:2003.11823 \[hep-ph\]](#).
- [58] K. Agashe, Y. Cui, L. Necib, and J. Thaler, [JCAP \*\*1410\*\*, 062 \(2014\)](#), [arXiv:1405.7370 \[hep-ph\]](#).
- [59] D. Kim, J.-C. Park, and S. Shin, [Phys. Rev. \*\*D100\*\*, 035033 \(2019\)](#), [arXiv:1903.05087 \[hep-ph\]](#).
- [60] M. Aoki and T. Toma, [JCAP \*\*1810\*\*, 020 \(2018\)](#), [arXiv:1806.09154 \[hep-ph\]](#).
- [61] J. Kopp, J. Liu, and X.-P. Wang, [JHEP \*\*04\*\*, 105 \(2015\)](#), [arXiv:1503.02669 \[hep-ph\]](#).

- [62] K. Kong, G. Mohlabeng, and J.-C. Park, *Phys. Lett.* **B743**, 256 (2015), [arXiv:1411.6632 \[hep-ph\]](#).
- [63] J. Berger, Y. Cui, and Y. Zhao, *JCAP* **1502**, 005 (2015), [arXiv:1410.2246 \[hep-ph\]](#).
- [64] E. Aprile *et al.* (XENON), (2020), [arXiv:2003.03825 \[physics.ins-det\]](#).
- [65] T. Bringmann and M. Pospelov, *Phys. Rev. Lett.* **122**, 171801 (2019), [arXiv:1810.10543](#).
- [66] Y. Ema, F. Sala, and R. Sato, *Phys. Rev. Lett.* **122**, 181802 (2019), [arXiv:1811.00520 \[hep-ph\]](#).
- [67] R. Essig *et al.* (2013) [arXiv:1311.0029 \[hep-ph\]](#).